The Sahara as a vicariant agent, and the role of Miocene climatic events, in the diversification of the mammalian order Macroscelidea (elephant shrews)

Christophe J. Douady[†‡], François Catzeflis[§], Jaishree Raman[¶], Mark S. Springer[‖††], and Michael J. Stanhope[†,††‡‡]

[†]Biology and Biochemistry, Queen's University of Belfast, 97 Lisburn Road, Belfast BT9 7BL, United Kingdom; [§]Institut des Sciences de l'Evolution, Université Montpellier 2, 34095 Montpellier, France; [¶]Department of Zoology, Göteborg University, Box 463, SE 405 30, Göteborg, Sweden; and [‖]Department of Biology, University of California, Riverside, CA 92521

Although the Sahara is a major geographical feature of the African continent, its role in the diversification of animal species is not well understood. We present here a molecular phylogeny for members of the endemic African mammalian order Macroscelidea (elephant shrews) with molecular-clock calculations; this molecular phylogeny provides convincing evidence that the genus *Elephantulus* is diphyletic. *Elephantulus rozeti*, the only elephant shrew species that resides north of the Sahara, is the sister group of a species from a different genus (*Petrodromus tetradactylus*), which resides just south of the Sahara. The split between these taxa coincided with major Miocene climatic events, which triggered the cooling and aridification of midlatitude continental regions, and a shift in the Sahara from a tropical to an arid environment. Thus, the North African distribution of *E. rozeti* is not the result of dispersion from an eastern species of the genus, but instead the result of a vicariant event involving the formation of the Sahara. The splitting events involved with most *Elephantulus* species in our analysis appear to coincide with these climatic events. This coincidence suggests that the environmental consequences associated with this period played an important role in the radiation of this order of mammals. The strongly supported phylogeny provides compelling evidence for a complex history of mosaic evolution, including pronounced bradytelic morphological evolution in some lineages, accelerated morphological evolution in others, and a remarkably slow rate of evolution of the male reproductive structure.

The Sahara Desert, which is clearly a barrier to animal dispersal, is a major geographical feature of the African continent. Detailed information regarding the possible role of the Sahara in establishing present-day animal species and distributions is lacking. The 15 living species of the mammalian order Macroscelidea (elephant shrews) are divided into four genera (*Rhynchocyon*, *Elephantulus*, *Macroscelides*, and *Petrodromus*), which are endemic to Africa. Only one species, *Elephantulus rozeti*, occurs north of the Sahara; other elephant shrews inhabit central, eastern, and southern parts of the continent (1). *E. rozeti* is presumed to have originated from an eastern species of *Elephantulus* that used the Nile Valley as a corridor for northward dispersal (1). In the view of Corbet and Hanks (1), morphological similarities that *E. rozeti* shares with other species in the genus preclude isolation of this taxon from other *Elephantulus* species before the Pleistocene epoch, 1.77 million years ago (MYA). Although there are morphologically based phylogenies for the order (1, 2), the evolutionary history of the members of this group is largely unexplored at the molecular level.

We investigated the evolutionary and biogeographic history of elephant shrews by using a phylogenetic approach. We employed several independent molecular loci that sampled 9 of the 15 elephant shrew species and at least one representative of all four genera. This phylogenetic perspective on elephant-shrew diversification was then examined in the context of relaxed molecular-clock calculations of evolutionary splitting events and information regarding climatic events of the period (3, 4) that were instrumental in the formation of the Sahara. The results highlight the previously unrecognized vicariant role of the Sahara in establishing the present-day distributions of the taxa within the order and emphasize the important role that Miocene climatic events had in shaping the evolutionary history of this African order of mammals. The phylogeny also serves to clarify earlier hypotheses regarding the overall history of the group and, in the process, provides evidence for mosaic patterns of morphological evolution, including bradytely (slow evolution) and tachytely (accelerated evolution).

Materials and Methods

Taxa and Phylogenetic Loci. At least one representative taxon of the four macroscelid genera, as well as 5–6 (depending on the phylogenetic locus) of the possible 10 species for the genus *Elephantulus*, were included in our analyses. Because of the highly surprising nature of our results regarding the evolutionary history of *Elephantulus rozeti*, the authenticity of this sample was positively verified with sequences derived from an independent sample. Given previous evidence for the inclusion of elephant shrews in the superordinal clade Afrotheria (5, 6), we used representative afrotherians as outgroups to Macroscelidea. The number of available outgroup sequences ranged from 5 to 10 for different loci (see Fig. 1 for species names associated with each locus). Molecular loci included the complete mitochondrial 12S rRNA, valine tRNA, and 16S rRNA genes and protein-coding segments of two nuclear genes [1.2 kb of exon 28 of von Willebrand factor (vWF); 1.2 kb of the 5′ region of exon 1 of interphotoreceptor retinoid binding protein (IRBP)]. Sequences for *Elephantulus brachyrhynchus* were obtained only for mitochondrial mtRNA because the degraded quality of the tissue sample did not allow amplification of the nuclear loci. Gene amplification and sequencing were performed as described (5, 7, 8). Sequence alignments were constructed according to the procedure suggested by Cassens *et al.* (9) and alignment-ambiguous positions were identified by using the software SOAP V1.1 (10). We used 25 different settings and gap penalties from 11 to 19 (steps of 2), extension penalties from 3 to 11 (steps of 2), and a criterion of 100% conservation across alignments for filtering out alignment-ambiguous sites. After we excluded re-
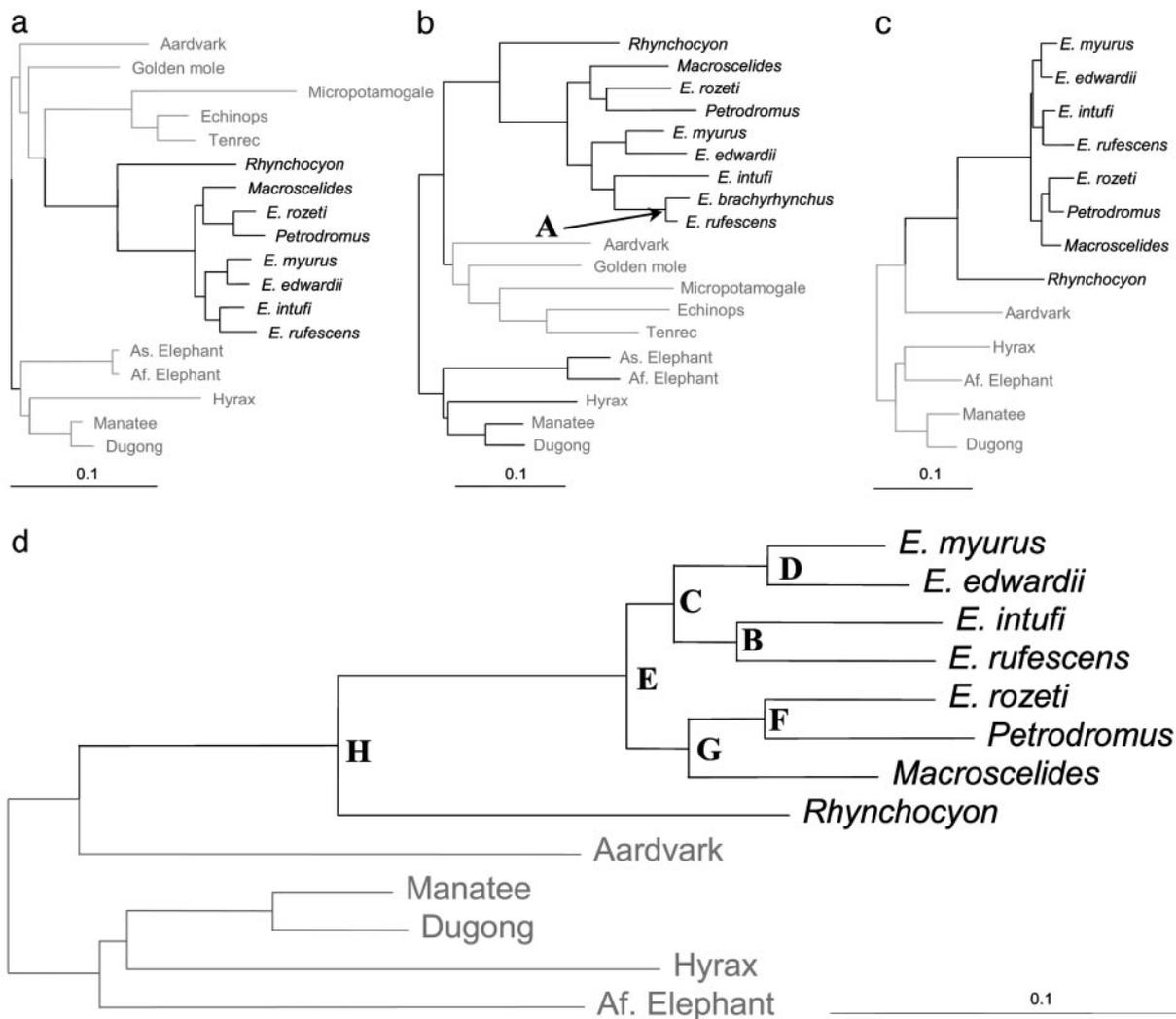
EVOLUTION

Fig. 1. ML trees for Macroscelidea based on sequences of vWF, −ln L = 5785.83804 (*a*); mtRNA, −ln L = 14359.20049 (*b*); IRBP, −ln L = 4498.62212 (*c*); and three-locus concatenation, −ln L = 20179.88633 (*d*). *E. brachyrhynchus* was sequenced for mtRNA only, because the poor quality of the sample prevented amplification of the nuclear loci. Support for nodes A–H is indicated in Table 1. Elephant shrews are shown in black and outgroup taxa are shown in gray. For convenience, trees were rooted to display the dichotomy between paenungulates and nonpaenungulates.

gions encompassing missing data for some taxa on 5′ and/or 3′ ends of the protein-coding loci, as well as ambiguous alignment positions in the mtRNA, the resulting sequence alignments were of the following lengths and numbers of taxa: mtRNA, 19 taxa for 2,141 positions; vWF, 18 taxa, 964 positions; IRBP, 13 taxa, 960 positions; concatenation of all three loci, 13 taxa and 4,065 positions, of which ≈53% were mitochondrial and 47% were nuclear. New sequences for vWF, IRBP, and mtRNA were obtained for *Rhynchocyon* sp. (GenBank accession numbers AY310887, AY310894, and AY310880), *Petrodromus tetradactylus* (AY310890, AY310897, and AY310883), *Macroscelides proboscideus* (AY310893, AY310900, and AY310886), *E. rozeti* (AY310888, AY310895, and AY310881), *Elephantulus myurus* (AY310889, AY310896, and AY310882), *Elephantulus intufi* (AY310891, AY310898, and AY310884), *Elephantulus edwardii* (AY310892, AY310899, and AY310885), and *Elephantulus brachyrhynchus* (AY310879; mtRNA only). Remaining sequences were extracted from GenBank.

Phylogenetic Reconstructions. MODELTEST (11) software was used to determine objectively the best-suited model of sequence evolution and the accompanying parameter values for each data set (base frequency, instantaneous rate for each substitution type, shape of the distribution used to accommodate the among-site rate variation, and proportion of invariant sites). The resulting models for each data set were as follows: mtRNA, general-time-reversible model of sequence evolution, plus gamma, plus invariant sites; vWF, Hasegawa–Kishino–Yano model of sequence evolution, plus gamma; IRBP, Kimura 2-parameter, plus gamma; concatenation, Tamura–Nei model of sequence evolution, plus gamma, plus invariant sites. All maximum-likelihood (ML) analyses used tree-bisection reconnection as the branch-swapping algorithm. ML bootstrapping was performed on 500 replicates of the data sets. Starting trees were obtained by stepwise addition.

Maximum parsimony (MP) used tree-bisection reconnection and the starting tree was obtained by stepwise addition with addition sequences 10× randomized. Minimum evolution (ME) was conducted by using both ML and log-determinant distances. Parameters for ML-distance calculations were the same as those for the ML search. Starting trees were obtained by stepwise addition. ME- and MP-bootstrap analyses both involved 500 replicates. MP, ME, and ML analyses were all conducted with PAUP* 4b8 (12).

Douady *et al.*

Bayesian phylogenetic analyses were performed with the Metropolis-coupled Markov chain Monte Carlo algorithm, implemented in MR. BAYES 2.01 (13). The tree space was explored by using four chains. We used a general-time-reversible model of sequence evolution allowing a gamma shape of among-site rate variation. Posterior probability distributions were obtained with the following prior distributions for the phylogeny and the parameters of the model of sequence evolution: branch length, uniform (0.0, 10.0); instantaneous-rate matrix, uniform (0.0, 100.0); base frequencies, Dirichlet (4.0); gamma shape, uniform (0.0, 10.0); proportion of invariant sites, uniform (0, 1). Proposal mechanisms for the Markov chains included attempted changes to the rate matrix (2.17%), base frequencies (2.17%), gamma shape (2.17%), proportion of invariant sites (2.15%), stochastic-nearest-neighbor interchanges (86.96%), and one worm change to the tree (4.35%). Random trees were used as seeds for each chain. We explored the tree space by using three independent runs of four chains with 1,000,000 generations, sampled every 100 generations. The number of generations to obtain convergence of the likelihood value for each data set, and thus the level at which "burn in" was set, were as follows: mtRNA, 16,000, 17,000, and 21,000 generations; vWF, 10,000, 11,000, and 13,000 generations; IRBP, 9,000, 8,000, and 9,000 generations; and concatenation, 15,000, 17,000, and 20,000 generations. Convergence was assessed empirically. The three independent runs yielded such similar results (SD < 0.0033) that only the first run is reported here.

The statistical significance of competing phylogenetic hypotheses (*Elephantulus* monophyly and alternatives to the best tree) were assessed under a likelihood model with the approximately unbiased (AU) test (14) as implemented in CONSEL 0.1f (15). The AU test is thought to be "approximately unbiased" compared with the earlier Shimodaira–Hasegawa test (16); in addition, it controls type I errors without reducing its power (i.e., without becoming over-conservative). Given the relative novelty of the AU test, for situations involving *a priori* hypotheses (17), we compared our results to *P* values obtained by the more classical Kishino–Hasegawa test (18), which is supplied also by CONSEL.

Timing. Divergence times were estimated from the concatenated data set by using the Bayesian relaxed molecular clock (19, 20), as implemented in the software DIVTIME, Version 5b (ftp:// statgen.ncsu.edu/pub/thorne). This method allows for multiple constraints on divergence times. As noted by Thorne and Kishino (21), it is important to include both minimum and maximum constraints to reduce the variance in estimated divergence dates. Following Springer *et al.* (22), we used a minimum of 54 million years and a maximum of 65 million years for the origin of Paenungulata. Branch lengths and the variance–covariance matrix were determined by a $F84 + \Gamma_8$ model (ESTBRANCHES, ftp://statgen.ncsu.edu/pub/thorne) and a topology corresponding to Fig. 1d that included a xenarthran (*Bradypus*) as an outgroup to Afrotheria (analyses with *Bradypus* resulted in precisely the same topology for afrotherians as shown in Fig. 1d). DIVTIME estimated the age of divergence and associated standard deviation for each node. The Markov chain was sampled 10,000 times with 100 cycles between each sample and after a burn in of 100,000 cycles. The prior values on the expected number of time units between the tip and root, the Brownian motion-constant ν, and the rate at the root were set at 80, 0.013, and 0.023, respectively. The accompanying standard deviations on these parameters were 40, 0.013, and 0.0011, respectively. The highest possible number of time units between the tip and root was set at 500 million years. The resulting date estimates, for the nodes comparably possible, showed a good correlation to those in Springer *et al.* (22), with estimates from either study included generally in the alternative-studies-credibility interval.

Results and Discussion

Phylogenetic Relationships. The resulting molecular phylogenies strongly highlight the relationships between the various species and genera (Fig. 1, Table 1). ML trees for the three independent and unlinked loci emerge in total agreement. Further, bootstrap percentages (MP, ME, ML) and posterior probabilities were high for most elephant shrew clades (Table 1). Exceptions included clades B (*E. intufi* + *Elephantulus rufescens*) and C (*Elephantulus* excepting *E. rozeti*) (Fig. 1) in MP and ME analyses with IRBP. Analyses with the concatenated data set resulted in uncommonly high bootstrap values for Macroscelidea and its subclades (MP = 94–100%; ME = 94–100%; ML = 9–100%). One of the most significant discrepancies between morphologically based phylogenies (1, 2) and our molecular data is the diphyly of the genus *Elephantulus*; this diphyly is clearly evident in the molecular topologies. The sister group to *E. rozeti* is, in fact, *Petrodromus tetradactylus*, rather than another species of *Elephantulus*. Bootstrap support for a grouping of *E. rozeti* and *Petrodromus* for the individual loci across a wide range of reconstruction methods is between 58% and 100% with a median at 97.5%. Support from the concatenated data set across methods was always >99%. Similarly, Bayesian analysis yields posterior probabilities of 0.98–1.0 (median at 1.0) for an association of *E. rozeti* and *Petrodromus*; however, it should be noted that there are studies indicating that posterior probability can sometimes overestimate clade strength support (23, 24). The competing hypothesis regarding the history of *E. rozeti*, *Elephantulus* monophyly, does not receive any support (Table 1). All statistical tests involving individual loci refute this association convincingly (*P* < 0.03) with rejection of *Elephantulus* monophyly involving the concatenated data set at *P* < 0.0002. Even more impressively, tests based on the concatenated data set reject any alternative to the most likely in-group association; the next most likely tree was rejected with *P* values of 0.0246 for the approximately unbiased test.

Divergence Times and the Sahara as a Vicariant Agent. The diphyly of the genus *Elephantulus* and a sister-group relationship between *E. rozeti* and *P. tetradactylus* provides a very different perspective on the historical biogeography of this group. *E. rozeti* is the only species of this group that inhabits the area north of the Sahara (Fig. 2) and is presumed to have attained this distribution by dispersal, originating from an eastern species of *Elephantulus* and traveling along the Nile valley. This hypothesis, as summarized by Corbet and Hanks (1), is primarily supported by (*i*) a morphological similarity with other species of *Elephantulus* that, in their opinion, precludes an isolation before the Pleistocene epoch (1.77 MYA) and (*ii*) van der Horst's (25) identification of the ancient Egyptian god Set as an elephant-shrew symbol, which argues for the presence of elephant shrews in northeast Africa in the recent past. The preferred molecular topology, however, refutes the possibility that *E. rozeti* is closely related to any of the east African species (for example, *E. rufescens*). Instead, we find very strong support for a close *E. rozeti*/*P. tetradactylus* association. Furthermore, molecular-clock calculations suggest an *E. rozeti*/*P. tetradactylus* split occurred around the mid- to late-Miocene boundary (11.6 MYA ± 2). Importantly, the present-day distributions of these two species are just north (*E. rozeti*) and south (*P. tetradactylus*) of the Sahara (Fig. 2). Available data indicate that the dryer and cooler climate of the mid-Miocene (3, 4), which followed the Neogene warmth climax [15–17 MYA (3, 4)], induced major changes in global climates (4), including aridification of midlatitude continental regions (4); these data suggest that the Sahara began its shift from a tropical to an arid environment around that time. Our molecular-clock determinations of the split between *E. rozeti* and *Petrodromus* coincide with this estimate of the Saharan aridifi-
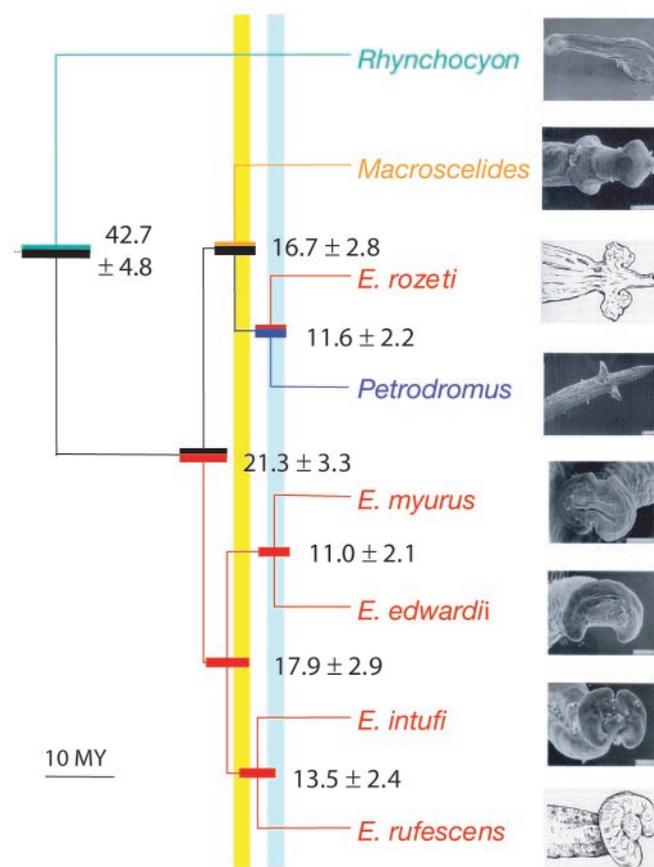
Table 1. Bootstrap and Bayesian probabilities for the proposed phylogeny

Analysis	A	B	C	D	E	F	G	H	F'
MP									
mtRNA	100	89	91	100	100	58	89	100	(0)
vWF	—	97	82	100	100	100	85	100	(0)
IRBP	—	(32)	(22)	97	100	89	91	100	(0)
Concatenation	—	98	94	100	100	99	95	100	(0)
ME ml									
mtRNA		98	99	100	100	84	90	98	(0)
vWF	—	99	44	97	100	100	80	100	(0)
IRBP	—	(11)	(7)	99	100	79	53	100	(0)
Concatenation	—	94	100	100	100	100	97	100	(0)
ME log-determinant									
mtRNA		90	99	100	100	60	98	89	(1)
vWF	—	100	61	100	100	100	95	100	(0)
IRBP	—	(36)	(15)	100	100	85	66	100	(0)
Concatenation	—	95	99	100	100	100	100	100	(0)
ML									
mtRNA	100	98	89	100	100	76	92	100	(0)
vWF	—	100	88	100	100	100	78	100	(0)
IRBP	—	79	55	98	100	96	95	100	(0)
Concatenation	—	100	98	100	100	100	100	100	(0)
MRBAYES									
mtRNA	1.00	1.00	1.00	1.00	1.00	0.98	1.00	1.00	(0.00)
vWF	—	1.00	0.98	1.00	1.00	1.00	0.89	1.00	(0.00)
IRBP	—	0.99	0.57	1.00	1.00	1.00	1.00	1.00	(0.00)
Concatenation	—	1.00	1.00	1.00	1.00	1.00	1.00	1.00	(0.00)

Clade columns are as follows: A, *E. brachyrhynchus*, *E. rufescens*; B, A + *E. intufi*; C, B + D; D, *E. myurus*, *E. edwardii*; E, C + G; F, *E. rozeti*, *P. tetradactylus*; G, F + *M. proboscideus*; H, E + *Rhynchocyon* (see Fig. 1). F' represents *Elephantulus* genus monophyly (i.e., C + *E. rozeti*). Parentheses indicate that node was not the best alternative.

cation and match very closely estimates of the formation of a major east-Antarctic ice sheet (ref. 3; Fig. 3) with its associated polar cooling. This cooling is hypothesized to have been a key trigger of the aridification of the midlatitude terrestrial biosphere (4). It seems likely, therefore, that the North African colonization by *E. rozeti* is not the result of a dispersion event, but instead the result of a fundamental vicariant event in which

Fig. 2. Macroscelidea distribution. The red arrow indicates the distribution for *E. rozeti*.

the Saharan aridification was instrumental. Importantly, the evolutionary splitting events that involve the other *Elephantulus* species in our analysis also appear to coincide with polar cooling and the establishment of the east-Antarctic ice sheet (Fig. 3); this coincidence suggests that this climatic event and its associated consequences may have played an important role in the *Elephantulus* radiation. Punctuated-equilibrium theory (26) predicts that the punctuated-speciation events occur through the normal process of allopatric speciation, which is caused by the disruption of organismal distributions into a series of peripherally isolated populations. We propose that the cooling period that followed the Neogene warmth climax altered many different African habitat types significantly and, as a consequence, disrupted elephant shrew population distributions. This disruption resulted in numerous evolutionary splitting events that coincide with this time period.

Implications of Molecular Data for the Evolution of Elephant Shrew Morphology. Parsimony analysis of morphological character matrixes have suggested the monophyly of the genus *Elephantulus* (2); there are, however, alternative morphological characters that may be much better markers of the true evolutionary history of the group. One particularly important example concerns the shape of the elephant shrew penis. Among six *Elephantulus* species investigated by Woodall (27), only *E. rozeti* differs in the shape of its glans penis; in addition, as pointed out by Woodall, the *E. rozeti* penis is very similar to that of *Petrodromus*, "with two lateral lobes and a narrowing distal end," whereas "in other species [of *Elephantulus*] examined the penis does not extend beyond the collar." Thus, even though *Petrodromus* and *E. rozeti* have nonreproductive morphologies that are quite different [*Petrodromus* differs from *Elephantulus* by a minimum of 12 characters, with 5 characters that are completely unique to that taxon (1)], they nonetheless have very similar male reproductive

Douady *et al.*

Fig. 3. Phylogenetic relationships and divergence time of elephant shrews. Respective penis morphologies are mapped onto the tree [drawings and electron micrographs from Woodall (10)]. The penis morphology of *E. brachyrhynchus* is highly similar to the other members of the genus, excluding *E. rozeti* (10). Tree scale is in millions of years and the picture scales represent 0.2 mm for *Rhynchocyon*, *Petrodromus*, and *Macroscelides*, and 1.0 mm for the remainder. Colors follow Fig. 2 coding. Horizontal rectangles stand for ± one standard deviation on divergence ages. Blue line indicates formation of east-Antarctic ice sheet and yellow line indicates Neogene warmth climax.

organs (Fig. 3). This similarity indicates that the structures have changed little since the two species shared a common ancestor.

The vicariant event associated with the aridification of the Sahara might also be an explanation for the similarity in reproductive structures of *Petrodromus* and *E. rozeti*. In such a vicariant scenario, there would not be strong selection for differentiation of reproductive structures related to the formation of interspecific hybrids because reproductive isolation would instead be afforded by the presence of an arid barrier to dispersal. However, there was clearly an increased rate of overall morphological evolution in *Petrodromus* as opposed to *E. rozeti*. We used PAUP* 4b8 and the morphological character matrix of Corbet and Hanks (1) to reconstruct the number of morphological changes on each of the *Petrodromus* and *E. rozeti* branches. When these results are considered along with our molecular-clock estimates, it is apparent that morphological evolution of *Petrodromus* was at least 2.5 times faster than that of *E. rozeti* (1.98 vs. 0.78 for deltran, and 2.41 vs. 0.34 for acctran, respectively). This analysis also supports the view that the last common ancestor of Macroscelidinae (node E in Fig. 1*d*) was more like living species of *Elephantulus* than either *Petrodromus* or *Macroscelides*. Thus, *E. rozeti* would have largely retained the ancestral morphology. It is important to realize that not only is this reconstruction the most parsimonious, but any alternative to

this scenario would necessitate the convergent evolution, within the *E. rozeti* lineage, of not one or two morphological characteristics, but instead, the overall body plan. Thus, it appears that *Petrodromus* has undergone significant change in morphology (suggesting directional selection on overall morphology in *Petrodromus*), although there has been selection to maintain the shape of the glans penis. After the split of *E. rozeti* and *Petrodromus*, *E. rozeti* was very clearly allopatric with regard to other elephant shrews, whereas *Petrodromus* was not (as based on present-day-, as well as fossil-record distributions). The fossil record indicates the presence of various elephant shrew taxa slightly before this proposed split south of the Sahara (Kenya, up to the Galana River), but not north of the Sahara (28). We propose that increased competition associated with overlapping distributions of the *Petrodromus* ancestor resulted in character displacement and rapid overall morphological change in this taxon; this morphological change did not occur in its sister species, *E. rozeti*, because of its resulting allopatric situation. The relative stasis in form of the *Petrodromus* glans penis may well have been associated with its being sufficiently distinct from the overlapping taxa (which presently includes *Rhynchocyon*, *E. brachyrhynchus,* and *E. rufescens*, Figs. 1*b*, 2, and 3) to act as an effective reproductive isolating mechanism. Thus, there was no directional selection for its change. *Petrodromus,* unlike *Elephantulus* and *Macroscelides,* live in "forest, thicket and the denser type of savanna woodland" (1). The accelerated morphological evolution of *Petrodromus* relative to *E. rozeti* might be related to the adaptation of *Petrodromus* to denser vegetation. The larger size of *Petrodromus* may represent an advantage in the denser undergrowth typified by such habitats.

Our molecular-clock estimates suggest that the *Elephantulus* body plan had its origins at least 21 ± 3 MYA (Fig. 3) and that the origins of the family (and of the order) are at least 43 ± 5 MY old (Fig. 3). The evolutionary history of elephant shrews involves both remarkable relative stasis in form (bearing in mind that earlier estimates had suggested *E. rozeti* was similar enough in form to other taxa of the genus to suggest that it had separated about 1.8 MYA) and, conversely, two cases of considerable diversification in form in *Petrodromus* and *Macroscelides*. It has been hypothesized elsewhere (29) that rhynchocyonines are typical of living fossils: they are members of a group of marked geologic longevity; they exhibit very little morphologic divergence from earlier members of the group; and they belong to a lineage that exhibits very low taxonomic diversity throughout most of its known history. In addition to providing further support to the view of rhynchocyonines as living fossils, now particularly evident because our estimate for their radiation is around 43 MYA, we would suggest that our data also support the view that bradytelic evolution is typical of at least some of the lineages within Macroscelidinae.

Surprisingly, this tendency toward morphological bradytelic evolution, typical of at least some of the elephant shrew lineages, is also typical of male genitalia in elephant shrews. Contrary to the flexible history previously proposed (27), with regard to the evolution of male reproductive structures in elephant shrews, our results suggest that the basic morphology was maintained over the course of the ≈11 million years since the separation of *Petrodromus* and *E. rozeti*, and was relatively consistent since the descent from the common ancestor of *E. edwardii*, *myurus*, *intufi*, *brachyrhynchus*, and *rufescens*, estimated at 18 ± 3 MYA (Figs. 1*b* and 3). This stasis is at odds with many other groups of mammals, including primates, rodents, and artiodactyls (30–34), in which male reproductive structures apparently evolve quite rapidly. It has been hypothesized elsewhere (27) that sexual selection on male genitalia might have led to rapid diversification in the morphology of male reproductive organs in elephant shrews. This rapid diversification hypothesis was based on the premise that *E. rozeti* was related more closely to other species of *Elephantulus* than to anything else. Our very strongly sup-

EVOLUTION

ported tree, however, argues for quite a different interpretation. The significant differences in morphology of elephant shrew male reproductive organs are between *Macroscelides* vs. *Petrodromus*/*E. rozeti*, as well as between the *Macroscelides*/*Petrodromus*/*E. rozeti* clade vs. the clade containing the remaining *Elephantulus* species (Fig. 3). Thus, although sexual selection might have been instrumental in creating those more ancient differences, strong stabilizing selection is a much better explanation for the striking similarity in the glans penis between the two morphologically different, but more recently separated taxa, *E. rozeti* and *Petrodromus*. We are not aware of any reported cases in mammals with such significant changes in overall morphology that coincide with little or no change in male reproductive structure. In fact, quite to the contrary, the literature regarding the evolution of male reproductive structures is rich with suggestions of rapid change in the morphology of the glans penis independent of overall body morphology, encompassing a wide range of mammalian groups (30–34).

Thus, it would seem the diversification of the order Macroscelidea represents a complex history of mosaic evolution, including pronounced bradytelic morphological evolution in some lineages, accelerated morphological evolution in others, and a remarkably slow rate of evolution of male reproductive structure. All of these phenomena fall within the backdrop of important climatic events of the mid-Miocene which appear to have been instrumental in shaping these particular features, as well as the overall history of this group.

1. Corbet, G. B. & Hanks, J. (1968) *Bull. Brit. Mus. (Nat. Hist.) Zool.* **16,** 47–111.
2. Corbet, G. B. (1995) *Mammal Rev.* **25,** 15–17.
3. Zachos, J., Pagani, M., Sloan, L., Thomas, E. & Billups, K. (2001) *Science* **292,** 686–693.
4. Flower, B. M. & Kennett, J. P. (1994) *Palaeogeogr. Palaeoclimatol. Palaeoecol.* **108,** 537–555.
5. Springer, M. S., Cleven, G. C., Madsen, O., de Jong, W. W., Waddell, V. G., Amrine, H. M. & Stanhope, M. J. (1997) *Nature* **388,** 61–64.
6. Stanhope, M. J., Waddell, V. G., Madsen, O., de Jong, W., Hedges, S. B., Cleven, G. C., Kao, D. & Springer, M. S. (1998) *Proc. Natl. Acad. Sci. USA* **95,** 9967–9972.
7. Porter, C. A., Goodman, M. & Stanhope, M. J. (1996) *Mol. Phylogenet. Evol.* **5,** 89–101.
8. Stanhope, M. J., Czelusniak, J., Si, J.-S., Nickerson, J. & Goodman, M. (1992) *Mol. Phylogenet. Evol.* **1,** 148–160.
9. Cassens, I., Vicario, S., Waddell, V. G., Balchowsky, H., Van Belle, D., Ding, W., Fan, C., Mohan, R. S. L., Simoes-Lopes, P. C., Bastida, R., *et al.* (2000) *Proc. Natl. Acad. Sci. USA* **97,** 11343–11347.
10. Löytynoja, A. & Milinkovitch, M. C. (2001) *Bioinformatics* **17,** 573–574.
11. Posada, D. & Crandall, K. A. (1998) *Bioinformatics* **14,** 817–818.
12. Swofford, D. L. (2002) PAUP*, Phylogenetic Analysis Using Parsimony (*and Other Methods) (Sinauer, Sunderland, MA), Version 4.0b10.
13. Huelsenbeck, J. P. & Ronquist, F. R. (2001) *Biometrics* **17,** 754–755.
14. Shimodaira, H. (2002) *Syst. Biol.* **51,** 492–508.
15. Shimodaira, H. & Hasegawa, M. (2001) *Bioinformatics* **17,** 1246–1247.
16. Shimodaira, H. & Hasegawa, M. (1999) *Mol. Biol. Evol.* **16,** 1114–1116.
17. Goldman, N., Anderson, J. P. & Rodrigo, A. G. (2000) *Syst. Biol.* **49,** 652–670.
18. Kishino, H. & Hasegawa, M. (1989) *J. Mol. Evol.* **29,** 170–179.
19. Thorne, J. L., Kishino, H. & Painter, I. S. (1998) *Mol. Biol. Evol.* **15,** 1647–1657.
20. Kishino, H., Thorne, J. L. & Bruno, W. J. (2001) *Mol. Biol. Evol.* **18,** 352–361.
21. Thorne J. L. & Kishino H. (2002) *Syst. Biol.* **51,** 689–702.
22. Springer, M. S., Murphy, W. J., Eizirik, E. & O'Brien, S. J. (2003) *Proc. Natl. Acad. Sci. USA* **100,** 1056–1061.
23. Suzuki, Y., Glazko, G. V. & Nei, M. (2002) *Proc. Natl. Acad. Sci. USA* **99,** 16138–16143.
24. Douady, C. J., Delsuc, F., Boucher, Y., Doolittle, W. F. & Douzery, E. J. (2003) *Mol. Biol. Evol.* **20,** 248–254.
25. van der Horst, C. J. (1946) *Trans. R. Soc. S. Afr.* **31,** 181–199.
26. Eldredge, N. & Gould, S. J. (1972) in *Models in Paleobiology*, ed. Schopf, T. J. M. (Freeman, Cooper, San Francisco), pp. 82–115.
27. Woodall, P. F. (1995) *J. Zool. (London)* **237,** 399–410.
28. Butler, P. M. (1995) *Mamm. Rev.* **25,** 3–14.
29. Novacek, M. (1984) in *Living Fossils*, eds. Eldredge, N. & Stanley, S. M. (Springer, New York), pp. 4–22.
30. Dixon, A. F. (1987) *J. Zool. (London)* **213,** 423–443.
31. Verrell, P. A. (1992) *Folia Primatol.* **59,** 114–120.
32. Lidicker, W. Z. J. (1968) *J. Mamm.* **49,** 609–643.
33. Contreras, L. C., Torresmura, J. C., Spotorno, A. E. & Catzeflis, F. M. (1993) *J. Mamm.* **74,** 926–935.
34. Walton, W. (1960) in *Physiology of Reproduction*, eds. Marshall, F. H. A. & Parkes, A. S. (Longman, London), Vol. 1, pp. 130–160.